Determination of the contribution of an imperfectly bonded inhomogeneity to macroscopic diffusivity

K.P. Frolova [1✉] [iD], N.M. Bessonov [1] [iD], E.N. Vilchevskaya [2] [iD]

[1] Institute for Problems in Mechanical Engineering RAS, St. Petersburg, Russia

[2] Flugsnapparegatan 6, Mölndal, Sweden

✉ fkp@ipme.ru

ABSTRACT
The paper contributes to the development of micromechanical approaches for determining the effective diffusivity of micro-heterogeneous materials, taking into account segregation, which is the accumulation of impurities at the phase interface. Two analytical approaches are investigated and compared with numerical simulation. In the first analytical approach, segregation is expressed in terms of a segregation parameter that prescribes the jump in concentration at the phase interface. In the second approach, an inhomogeneity with an ultra-thin mass isolating coating is introduced, and segregation is expressed in terms of equivalent surface resistivity. The developed numerical method considers inhomogeneities with an outer weakly permeable shell of thickness that tends to zero. Comparison among various models made it possible to estimate their limitations and perspectives.

KEYWORDS
effective properties • imperfect contacts • segregation • diffusion • homogenization problem

Introduction

Determination of the effective diffusivity of micro-heterogeneous materials is one of advanced problems in mechanics. Indeed, the internal structure of a material affects its permeability and, as a result, the total amount of a diffusing substance. The accumulation of harmful impurities, in turn, can lead to the degradation of the mechanical properties of materials [1–5]. Therefore, a comprehensive analysis of the influence of microstructure on macroscopic diffusivity is of great importance. One of the problems of fundamental interest in this area is the issue of accounting for segregation that is accumulation of impurities along the phase interface [6,7]. Typically, the effective properties of various natures are determined within classical micromechanical approaches, which assume that fields at the phase interface are continuous. However, the presence of segregation disrupts the continuity of the concentration field at the internal boundaries of heterogeneous materials [8]. In this case, the phase interface becomes "imperfect" and surface effects must be taken into account [9,10].

Only a small number of works are dedicated to accounting for the presence of imperfect contacts at the phase interface within micromechanical models. In [9,11–16], diffusivity problem was investigated and segregation was accounted for in terms of a

segregation parameter, which is the ratio of concentrations on the outer and inner sides of the inhomogeneity boundary. Thus, in this approach, a jump in concentration across the phase interface is prescribed. In [12,13], the segregation parameter was introduced in the modified effective media homogenization method. In [14,16], it was incorporated into effective field methods expressed in terms of property contribution tensors that reflect the contribution of individual inhomogeneities to the property of interest. Another approach to account for imperfect interfaces involves considering inhomogeneities with an interface possessing extreme properties. Usually such an approach is used within conductivity problem [9,17–25]. Within the approach some models express jump in the field in terms of surface conductivity [17–22], whereas another models consider an ultra-thin outer shell and realize limit transitions [9,23–25]. Note that in the context of the diffusivity process accompanied by segregation, the coating should function as an insulator. Consequently, segregation can be expressed within this approach in terms of equivalent surface diffusion resistivity. The question of the most appropriate approach to account for segregation remains open.

The problem of analytical determination of effective diffusivity consists of two parts: solution of one-particle problem and application of this solution within some homogenization scheme to account for the presence of multiple inhomogeneities [26]. The problem of a single inhomogeneity placed in an infinite matrix is known as the (second) Eshelby problem [27], which originally refers to elasticity under assumption on perfect phase interfaces. Solution of the Eshelby problem for conductivity in the case of perfect contacts was derived by Fricke [28].

In general, the presence of imperfect phase interfaces must be taken into account at both steps. In [29,30], we compared the analytical solution of the first part of the problem obtained using two aforementioned approaches for accounting for imperfect contacts: the approach in which segregation is expressed in terms of a segregation parameter and the approach in which segregation is expressed in terms of equivalent surface resistivity. In particular, it was shown that, for certain parameters of the internal structure, the results obtained within the two approaches exhibit significant qualitative differences that can be quite consequential. A detailed investigation of these differences was beyond the scope of papers [29,30]. In the present research, we further develop the numerical method to account for imperfect contacts and compare the analytical solutions with the numerical results. Such a comparison could facilitate an analysis of the qualitative differences between the two analytical approaches and help in answering the question of which approach is most accurate. Additionally, numerical simulation may help in overcoming difficulties related to the complexity of solving the problem for inhomogeneities with a non-spherical shape and, more generally, with non-ellipsoidal shapes. Unlike spherical inhomogeneities, ellipsoidal and even spheroidal inhomogeneities have imperfect interfaces of non-constant curvature, which complicates the introduction of an outer shell of constant thickness within the corresponding analytical approach, making it less physically justifiable. Furthermore, an analytical solution for a single inhomogeneity embedded in an infinite matrix exists only for ellipsoidal inhomogeneities. However, considering irregular shapes is often necessary for accurately modeling real materials.

Single inhomogeneity problem

Effective properties of micro-heterogeneous materials can be expressed in terms of various microstructural parameters. In the present research, we follow [26] and consider property contribution tensors, the sum of which serves as a relevant microstructural parameter reflecting the contributions of individual inhomogeneities to the macroscopic property of interest. This takes into account physical and geometrical characteristics of inhomogeneities, such as properties, shape, and orientation in the matrix. The property contribution tensor is to be derived from the solution of the single inhomogeneity problem, while the effective properties of the material can be determined using a homogenization scheme written in terms of the corresponding microstructural parameters. We will focus on the first part of the problem of determining effective properties by introducing the diffusivity contribution tensor of a single ellipsoidal inhomogeneity with an imperfect boundary.

Let us consider the representative volume element (RVE) *V,* which is a typical point of continuum at the macro level, consisting of an isotropic ellipsoidal inhomogeneity with volume $V_1 << V$ and diffusivity $\mathbf{D}_1 = D_1 \mathbf{I}$, along with an isotropic matrix with diffusivity $\mathbf{D}_0 = D_0 \mathbf{I}$. We seek the solution of a stationary diffusion problem in the absence of inner sources and under the assumption on linear constitutive relations in each phase of the heterogeneous material:

$$\nabla \cdot \mathbf{J}(\mathbf{r}) = 0, \ \mathbf{J}(\mathbf{r}) = -\mathbf{D}(\mathbf{r}) \cdot \nabla c(\mathbf{r}), \tag{1}$$

where $\mathbf{r}$ is the position vector, $\mathbf{J}$ is the diffusion flux, c is the concentration, $\mathbf{D}(\mathbf{r}) = D_0 \mathbf{I}$ if $\mathbf{r}$ belongs to the matrix and $\mathbf{D}(\mathbf{r}) = D_1 \mathbf{I}$ if $\mathbf{r}$ is in the inhomogeneity.

The macroscopic properties must be independent on the type of the boundary conditions (BCs) prescribed on the boundary Σ of the RVE. Therefore, any BCs can be used. It is convenient to work with uniform BCs within analytical approaches. In the case of prescribed concentration, these are defined as follows:

$$c(\mathbf{r})|_\Sigma = \mathbf{G}_0 \cdot \mathbf{r}, \tag{2}$$

where $\mathbf{G}_0$ is a constant vector. $\mathbf{G}_0$ also represents a uniform field that would exist everywhere in the RVE in the absence of inhomogeneity. In this case, first, effective properties are automatically compatible with their definition in energy terms [26], and second, the averaged concentration gradient coincides with $\mathbf{G}_0$ ($\langle \nabla c(\mathbf{r}) \rangle_V = \mathbf{G}_0$). In the same manner, one could consider uniform BCs for the normal component of the flux.

We assume that the material satisfies linear constitutive relations, so the flux and concentration gradient at the continuum point are related by classical Fick's law through the effective diffusivity tensor $\mathbf{D}^{eff}$:

$$\langle \mathbf{J} \rangle_V = -\mathbf{D}^{eff} \cdot \langle \nabla c \rangle_V, \tag{3}$$

here $\langle \dots \rangle_V = \int_V \dots dV$ denotes averaging over the RVE, and the averaged field values correspond to values at a continuum point at the macro-level.

In the linear case, the volume average of the diffusion flux can be represented as follows [14]:

$$\langle \mathbf{J} \rangle_V = -\mathbf{D}_0 \cdot \mathbf{G}_0 + \Delta\mathbf{J}, \tag{4}$$

where $\Delta\mathbf{J}$ is an additional flux caused by the presence of the inhomogeneity that can be expressed in terms of the diffusivity contribution tensor $\mathbf{H}$ such that

$$\Delta\mathbf{J} = -\frac{V_1}{V} \mathbf{H} \cdot \mathbf{G}_0. \tag{5}$$

Hence,

$$\mathbf{D}^{eff} = \mathbf{D}_0 + \frac{V_1}{V}\mathbf{H},$$ (6)

here the effective diffusivity tensor can generally be orthotropic. In the case of isotropy of the phases' material, the overall anisotropy is induced solely by the shape of the inhomogeneity. Specifically, for ellipsoidal shapes, the tensor is orthotropic; for spheroidal shapes, it exhibits transverse isotropy; and it becomes isotropic in the case of a sphere.

Diffusivity contribution tensors of inhomogeneities with imperfect contacts caused by segregation, modeled in different ways, differ from one another. We will now discuss a few mathematical models of imperfect contact and introduce corresponding property contribution tensors.

Diffusivity contribution tensors

Within the framework of the present paper, we consider two analytical approaches for modeling segregation. The first approach involves prescribing a jump in the concentration field, while the second approach considers an inhomogeneity with an ultra-thin isolating coating. For further details, we refer to our previous works [16,29,30] as well as the works of Levin and Markov [24,25]. Below, we briefly outline the main ideas and provide the key formulas associated with each approach.

In both analytical approaches, the diffusivity contribution tensor can be expressed in terms of the concentration tensor of concentration gradient $\mathbf{\Lambda}$, which linearly relates the field inside the inhomogeneity to the applied one ($\nabla c(\mathbf{r}) = \mathbf{\Lambda}(\mathbf{r}) \cdot \mathbf{G}_0$ when $\mathbf{r}$ belongs to inhomogeneity). The presence of imperfect contacts must be considered at two stages within the homogenization problem: during the averaging of fields as presented in Eq. (3), and when calculating the concentration tensor. Both the averaging procedure and the determination of the concentration tensor are influenced by the geometry of the internal boundaries and the boundary conditions applied to them. Consequently, the property contribution tensors obtained within the two approaches are expressed in terms of different variables that account for the effects of imperfect contacts.

In the first analytical approach to accounting for imperfect contacts, the influence of these contacts is modeled using a segregation parameter s_c, defined as the ratio of the concentration values on the outer and inner sides of the interface Γ between the matrix (+) and the inhomogeneity (-). The geometry of the inhomogeneity in the ($\mathbf{e}_1$, $\mathbf{e}_3$) plane is shown in Fig. 1. So, the following boundary conditions hold:

$$D_0 \left.\frac{\partial c(\mathbf{r})}{\partial n_\Gamma}\right|_{r \to \partial\Gamma+} = D_1 \left.\frac{\partial c(\mathbf{r})}{\partial n_\Gamma}\right|_{r \to \Gamma-}, c(\mathbf{r})|_{r \to \Gamma+} = s_c c(\mathbf{r})|_{r \to \Gamma-},$$ (7)

where $\mathbf{n}_\Gamma$ is the outer normal vector to Γ. Note that the jump in concentration can be calculated as $[c] = (s_c - 1)c(\mathbf{r})|_{r \to \Gamma-}$.

The averaged fields are as follows:

$$\langle \nabla c \rangle_V = \left(1 - \frac{V_1}{V}\right)\langle \nabla c \rangle_{V_0} + s_c \frac{V_1}{V}\langle \nabla c \rangle_{V_1}, \langle \mathbf{J} \rangle_V = \left(1 - \frac{V_1}{V}\right)\langle \mathbf{J} \rangle_{V_0} + \frac{V_1}{V}\langle \mathbf{J} \rangle_{V_1},$$ (8)

here $\langle ... \rangle_{V_0} = \int_{V_0} ... dV_0$ represents the averaging over the volume V_0 of the matrix, while $\langle ... \rangle_{V_1} = \int_{V_1} ... dV_1$ denotes the averaging over the volume of the inhomogeneity.

Diffusivity contribution tensor can be found then by the following equation:

$$\mathbf{H} = (D_1 - s_c D_0)\mathbf{\Lambda}_c, \tag{9}$$
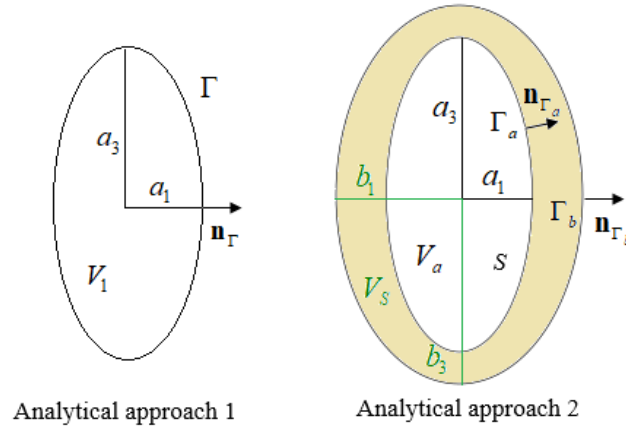
where constant concentration tensor $\mathbf{\Lambda}_c$ ($\langle \nabla c \rangle_{V_1} = \mathbf{\Lambda}_c \cdot \mathbf{G}_0$) of an ellipsoidal inhomogeneity is as follows:

$$\mathbf{\Lambda}_c = \sum_{j=1}^{3} \frac{1}{s_c\left(1 + A_j\left(\frac{D_1}{s_c D_0} - 1\right)\right)} \mathbf{e}_j \mathbf{e}_j, \tag{10}$$

here

$$A_j = a_1 a_2 a_3 \int_0^{\infty} \left(p + a_j^2\right)^{-1} / \left(2\sqrt{(p + a_1^2)(p + a_2^2)(p + a_3^2)}\right) dp, \tag{11}$$

where a_1, a_2, a_3 are the lengths of the semi-axes of the ellipsoidal inhomogeneity.

Fig. 1. Geometry of inhomogeneity considered in two analytical approaches

In the second analytical approach to accounting for imperfect contacts, a two-component layered ellipsoid is introduced (as shown in Fig. 1 in the ($\mathbf{e}_1$, $\mathbf{e}_3$) plane). The diffusivity of the inner ellipsoid coincides with that of the original inhomogeneity, while diffusivity of the outer layer, denoted as D_s, differs (material of the layer is assumed to be isotropic). The lengths of the semi-axes of the inner and outer ellipsoids, represented as a_1, a_2, a_3 and b_1, b_2, b_3, respectively, are related through a constant component ξ associated with confocal ellipsoids as:

$$b_i^2 = a_i^2 + \xi. \tag{12}$$

The bounds Γ_a of the inner ellipsoid and Γ_b of the outer ellipsoid are assumed to be perfect, so fields are continuous:

$$\left. D_0 \frac{\partial c(\mathbf{r})}{\partial n_{\Gamma_b}} \right|_{r \to \partial \Gamma_b+} = \left. D_s \frac{\partial c(\mathbf{r})}{\partial n_{\Gamma_b}} \right|_{r \to \Gamma_b-}, \left. c(\mathbf{r}) \right|_{r \to \Gamma_b+} = \left. c(\mathbf{r}) \right|_{r \to \Gamma_b-}$$

$$\left. D_s \frac{\partial c(\mathbf{r})}{\partial n_{\Gamma_a}} \right|_{r \to \partial \Gamma_a+} = \left. D_1 \frac{\partial c(\mathbf{r})}{\partial n_{\Gamma_b}} \right|_{r \to \Gamma_a-}, \left. c(\mathbf{r}) \right|_{r \to \Gamma_a+} = \left. c(\mathbf{r}) \right|_{r \to \Gamma_a-} \tag{13}$$

The thickness of the outer shell of the two-component layered ellipsoid is assumed to tend to zero that is modeled by letting $\xi \to 0$. This extremely thin coating is considered to be an isolator, resulting in $D_s \to 0$. Consequently, it becomes convenient to express the imperfect contact in terms of the equivalent surface diffusion resistivity β:

$$\beta = \frac{V_s}{D_s S} = \frac{4\pi(a_1^2 a_2^2 + a_1^2 a_3^2 + a_2^2 a_3^2)}{6 a_1 a_2 a_3 S} \lim_{\xi \to 0, D_s \to 0} \frac{\xi}{D_s}, \tag{14}$$

where V_s is the volume of the outer shell, S is the surface area of the inner ellipsoid (see Fig. 1). In the specific case of a spherical inhomogeneity, where $a_1 = a_2 = a_3 = a$, Eq. (14)

simplifies to $\beta = \lim\limits_{\delta \to 0, D_s \to 0} \delta/D_s$, where δ is a constant thickness of the outer shell that tends to zero.

The averaged fields are as follows:

$$\langle \nabla c \rangle_V = \left(1 - \frac{V_1 + V_S}{V}\right) \langle \nabla c \rangle_{V_0} + \frac{V_1}{V} \langle \nabla c \rangle_{V_a} + \frac{V_S}{V} \langle \nabla c \rangle_{V_S},$$

$$\langle \mathbf{J} \rangle_V = \left(1 - \frac{V_1 + V_S}{V}\right) \langle \mathbf{J} \rangle_{V_0} + \frac{V_1}{V} \langle \mathbf{J} \rangle_{V_a} + \frac{V_S}{V} \langle \mathbf{J} \rangle_{V_S} \qquad (15)$$

here $\langle ... \rangle_{V_a} = \int_{V_S} ... dV_a$ and $\langle ... \rangle_{V_S} = \int_{V_S} ... dV_S$ denotes the averaging over the volume of the inner ellipsoid and over the outer shell respectively.

Diffusivity contribution tensor can be found as:

$$\mathbf{H} = (D_1 - D_0)\mathbf{\Lambda}_a - \frac{V_S}{V_a} D_0 \mathbf{\Lambda}_s, \qquad (16)$$

where constant concentration tensors $\mathbf{\Lambda}_a$ ($\langle \nabla c \rangle_{V_a} = \mathbf{\Lambda}_a \cdot \mathbf{G}_0$) and $\mathbf{\Lambda}_s$ ($\langle \nabla c \rangle_{V_S} = \mathbf{\Lambda}_s \cdot \mathbf{G}_0$) are as follows:

$$\mathbf{\Lambda}_a = D_0 \sum_{j=1}^3 \frac{1}{A_j D_1 + (1 - A_j)D_0 + (1 - A_j)D_0 D_1 \beta\left(A_j - \frac{F_j}{H}\right)} \mathbf{e}_j \mathbf{e}_j,$$

$$\mathbf{\Lambda}_s = \sum_{j=1}^3 A_j \frac{D_1}{D_s} \mathbf{\Lambda}_{a_{jj}} \mathbf{e}_j \mathbf{e}_j \qquad (17)$$

here $H = \frac{a_1^2 a_2^2 + a_1^2 a_3^2 + a_2^2 a_3^2}{2 a_1^2 a_2^2 a_3^2}$, $F_1 = \dfrac{\left(\sum_{k=1}^3 a_k^{-2}\right)A_1 - \frac{a_1 a_2 a_3}{2} \int_0^\infty \dfrac{3(p+a_2^2)(p+a_3^2) + (p+a_1^2)(p+a_2^2) + (p+a_1^2)(p+a_3^2)}{\sqrt{(p+a_1^2)^5 (p+a_2^2)^3 (p+a_3^2)^3}} dp}{2}$,

expressions for F_2 and F_3 can be obtained by the last equation with appropriate permutation of indices.

In our paper [30], we compared the two analytical approaches discussed above. It was shown that they yield the same result only in the case of spherical inhomogeneity, specifically when $a_1 = a_2 = a_3 = a$. In this scenario, the segregation parameter s_c and the equivalent surface resistivity β are related by the equation: $s_c = 1 + D_1 \beta / a$.

Let us now discuss the numerical approach for accounting for segregation. In this approach, we consider an inhomogeneity with a mass-isolating coating representing a shell. The procedure for numerically solving Eq. (1) for concentration is described in Appendix A. The diffusivity contribution tensor is determined through the effective diffusivity based on Eq. (6). The effective diffusivity tensor, in turn, is calculated from the solution of the following system of equations:

$$\begin{cases} \langle \mathbf{J} \rangle_1 = -\mathbf{D}^{eff} \cdot \langle \nabla \mathbf{c} \rangle_1, \\ \langle \mathbf{J} \rangle_2 = -\mathbf{D}^{eff} \cdot \langle \nabla \mathbf{c} \rangle_2, \\ \langle \mathbf{J} \rangle_3 = -\mathbf{D}^{eff} \cdot \langle \nabla \mathbf{c} \rangle_3, \end{cases} \qquad (18)$$

here the indices 1, 2, 3 correspond to three calculations where the linear boundary condition (2) is alternately applied along three mutually orthogonal directions $\mathbf{e}_1$, $\mathbf{e}_2$, $\mathbf{e}_3$ (here $\mathbf{e}_1$, $\mathbf{e}_2$, $\mathbf{e}_3$ are unit vectors aligned with semi-axes of the ellipsoidal inhomogeneity. Note that the equalities $\langle \nabla c \rangle_j = \mathbf{G}_0$ are satisfied automatically for j =1, 2, 3 respectively.

To find the effective diffusivity, we multiply Eq. (18) by $\mathbf{e}_1$, $\mathbf{e}_2$, $\mathbf{e}_3$ respectively and then sum them. This leads to the following equality:

$$\mathbf{D}^{eff} = -\left(\left(\sum_{j=1}^3 \mathbf{e}_j \langle \nabla c \rangle_j\right)^{-1} \cdot \sum_{j=1}^3 \langle \mathbf{J} \rangle_j \mathbf{e}_j\right)^{\mathbf{T}}. \qquad (19)$$

Within the numerical approach we consider different shapes for the outer shell:

1. The outer shell is represented by two ellipsoids (Numerical method 1).

2. The outer shell is characterized by a constant thickness (Numerical method 2).

Let us further discuss these methods.

In the case of Numerical method 1, when the semi-axes of the inner and outer ellipsoids are related by Eq. (12), the numerical solution can be directly compared with the corresponding analytical solution. However, consideration of such a shape of the outer shell is meaningful only within analytical approach based on the solution of a single inhomogeneity problem for confocal ellipsoids. Additionally, within the numerical approach, we examine a second case where the semi-axes of the two ellipsoids are related as $b_i = a_i + \delta$, with δ being a constant. To facilitate the comparison of the two numerical solutions, we relate the parameter ξ introduced in the first case to the parameter δ introduced in the second case in the following way:

$$\xi = \delta(2a_{max} + \delta), \tag{20}$$

where a_{max} corresponds to the largest semi-axis. In the case of confocal ellipsoids, δ represents the minimum value of the thickness of the outer shell.

In the case of Numerical method 2, the inner figure is an ellipsoid, while the outer one is not. This model is particularly significant for materials containing inhomogeneities with real coatings of finite thickness. At the same time, even in scenarios involving an ultra-thin coating used to model segregation, the model offers advantages, as in this case the thickness δ approaches zero, rather than ξ, making it a more physically relevant representation. To compare the two numerical methods, we relate δ and ξ using Eq. (20). The technical complexity associated with forming a layer of constant thickness arises from the need to calculate the distance between the surface of the ellipsoid and any point outside it to determine whether that point belongs to the layer [31,32]. The proposed method for solving this problem is described in Appendix B.

To simulate a micro-heterogeneous material in Numerical methods 1 and 2, we create three types of cubic cells based on the material they represent: inhomogeneity, layer, or matrix. When the thickness of the isolating layer approaches zero, matrix cells and inhomogeneity cells can become neighbors, resulting in no isolating cells between them. This situation gives rise to the issue of "penetration" which violates isolation. To avoid the "penetration" problem, we must consider a layer of finite thickness that, in fact, does not accurately model segregation on a real ultra-thin phase interface. To accurately simulate the case of an ultra-thin coating of interest, we propose to extrapolate the dependencies of the components of the diffusivity contribution tensor on ξ (or δ) and estimate the values at $\xi = 0$ (or $\delta = 0$).

In conclusion, we would like to emphasize that the consideration of an isolating coating—both in analytical models and numerical methods—allows the modeling of impurity accumulation solely outside the inhomogeneities. On the other hand, prescribing a jump in concentration enables the modeling of impurity accumulation in both the exterior and interior of the inhomogeneities. Segregation typically occurs along grain boundaries and within pores. In the first case, it is essential to model the grains as inhomogeneities and the grain boundaries as the matrix when employing the isolating coating approach (as opposed to modeling grains as the matrix and grain boundaries as inhomogeneities). Notably, this approach cannot be applied to model segregation in the case of pores at all.

Results and Discussion

We calculate the diffusivity contribution tensor of a less mass-conductive inhomogeneity with an imperfect boundary, which is embedded in a more mass-conductive matrix. This approach allows us to model segregation in polycrystalline materials within the framework of all the investigated models (where grains are modeled as inhomogeneities, and grain boundaries are modeled as the matrix, with segregation occurring along the grain boundaries). Inhomogeneity is assumed to have the shape of a prolate spheroid (where $a_1 = a_2 = a$ and $\gamma = a_3/a > 1$) or a sphere (where $a_1 = a_2 = a_3 = a$ and $\gamma = 1$).

To compare the results obtained within the framework of two investigated analytical approaches for accounting for imperfect contacts, we relate the segregation parameter s_c, which is responsible for the jump in concentration, to the equivalent surface resistivity β, which accounts for the surface effect in the following manner:

$$s_c = 1 + R, \quad R = \frac{D_1 \beta}{a} = \frac{D_1(1+2\gamma^2)}{3a^2\gamma\left(1+\frac{\gamma^2}{\sqrt{\gamma^2-1}}\arcsin\frac{\sqrt{\gamma^2-1}}{\gamma}\right)} \lim_{\xi\to 0, D_s\to 0} \frac{\xi}{D_s}, \tag{21}$$

since in this case the application of both analytical approaches leads to the same result [29].

An ultra-thin isolating coating emerges when $\xi \to 0$ and $D_s \to 0$. The ratio $\lim_{\xi\to 0, D_s\to 0} \xi/D_s$ and the parameter R introduced in accordance with Eq. (21) are constant values. As discussed in the previous section, direct consideration of $\xi \to 0$ in numerical method presents technical challenges. To compare the numerical solution with the analytical ones, we evaluate the numerical solution at several small values of ξ while keeping ξ/D_s constant, and then we extrapolate the results.

We start with calculating the components of diffusivity contribution tensor of a spherical inhomogeneity (when $\gamma = 1$). In this case, not only do both analytical approaches yield the same result, but all numerical methods do as well, since the thickness of the coating remains constant along the inhomogeneity border. Specifically, we consider a material with a ratio of the diffusion coefficient of the inhomogeneity to that of the background matrix given by $\alpha = D_1/D_0 = 0.1$.

Figure 2 shows the dependence of the components of the diffusivity contribution tensor of a spherical inhomogeneity with imperfect contact on δ, which remains constant along the phase interface, at a constant ratio ξ/D_s. Note that in this case, an ultra-thin coating emerges when $\delta \to 0$. It is seen that for small values of the thickness of the outer shell, the dependencies can be well approximated by linear functions. The results are extrapolated to facilitate the limit transition. The numerical and analytical results are found to be in close agreement, with an error of less than 1 %. Additionally, in the absence of the coating, the components of the property contribution tensor calculated both analytically and numerically yield $H_{11} = H_{22} = H_{33} \approx 1.3$. Thus, in all models – both analytical and numerical – increasing R enhances the "negative" contribution of low mass-conducting inhomogeneities, meaning that the presence of such inhomogeneities will decrease macroscopic mass permeability.
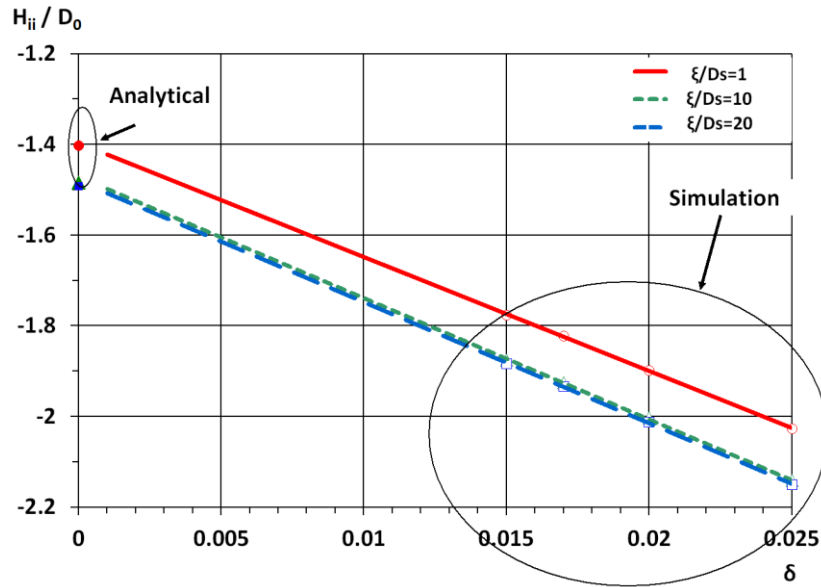
Fig. 2. Extrapolation of the numerical dependencies of the components of the diffusivity contribution tensor with respect to the thickness of the outer shell

We now turn our attention to spheroidal inhomogeneities. As previously mentioned, the two analytical approaches yield different results for any relationship between the segregation parameter s_c and equivalent surface resistivity β. Consequently, a quantitative comparison of the results is not particularly valuable. However, the qualitative differences are significant.
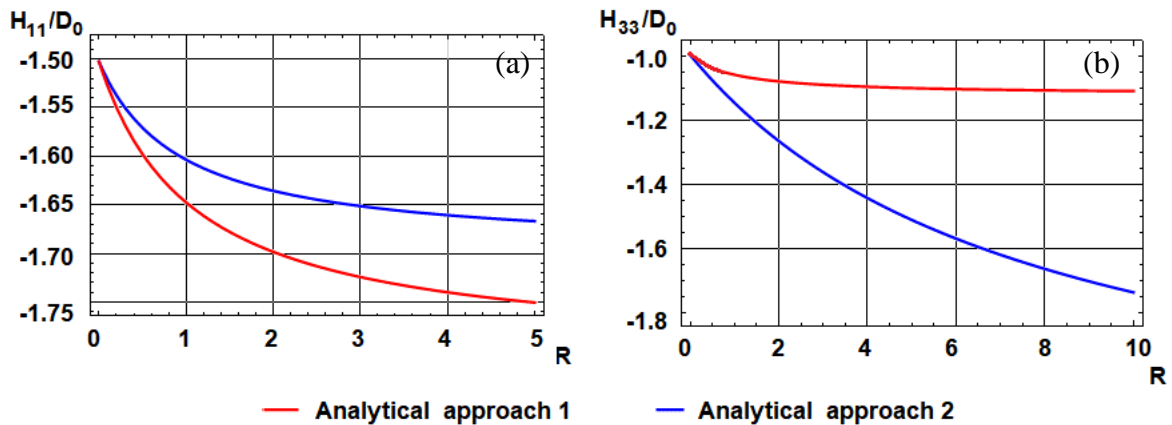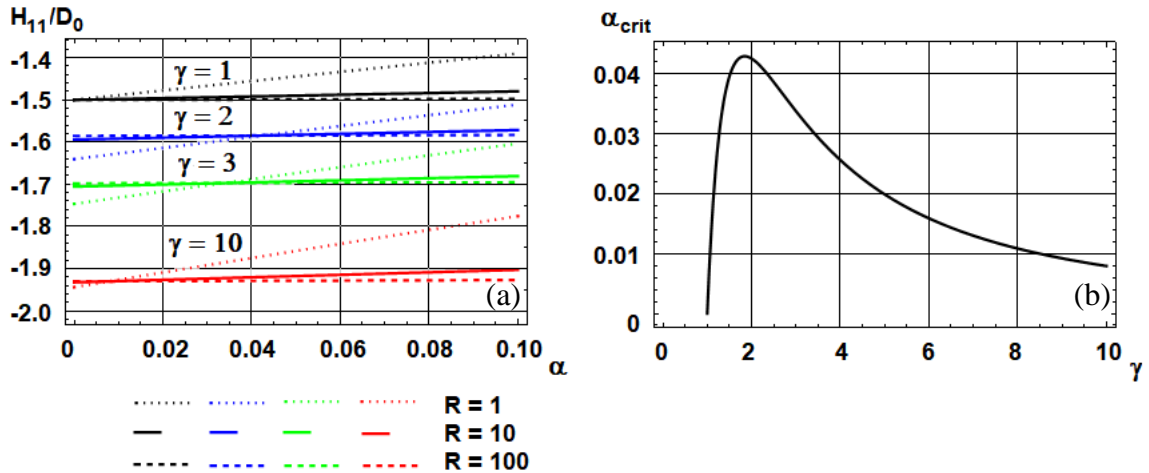

Fig. 3. Dependencies of the dimensionless components of the diffusivity contribution tensor H_{11}/D_0 (a) and H_{33}/D_0 (b) with respect to the parameter R

According to [26], the increase in the dimensionless parameter R, introduced by Eq. (21) and indicative of an imperfect contact, impacts the results obtained through the two analytical approaches in different ways. When R is unknown, the application of one approach allows for a border range of values for H_{ii} and, consequently, for effective properties. This can be critical when comparing theoretical results with experimental data. Note that both approaches – Analytical approach 1, which accounts for an imperfect contact via a jump prescription, and Analytical approach 2, which considers imperfect contact through an isolating coating – can yield a wider range of the results than the

other, depending on the internal structure parameters. For instance, as shown in Fig. 3, at γ = 3 and α = 0.1, the increase in R affects H_{33} calculated using Analytical approach 2 significantly more than it does in Analytical approach 1. However, the influence on H_{11} is comparatively less. Notably, the difference in H_{33} calculated by the two approaches is greater than in H_{11}.

There is another significant qualitative difference between the two analytical approaches. In Analytical approach 1, the magnitudes of all components of the diffusivity contribution tensor increase with an increasing R, which is physically justified. This is because the degradation of mass permeability in the inhomogeneity should enhance its contribution to the effective properties of a material comprised of less mass-conducting inhomogeneities and a more mass-conducting matrix. In contrast, in Analytical approach 2, for certain values of the inner structure parameters, an opposing trend occurs. In Fig. 4(a) it is shown that for a given γ, the magnitude of the component H_{11} decreases with increasing R when $\alpha < \alpha_{crit}$ (where α_{crit} represents some "critical" value). An increase in γ leads to a decrease in α_{crit}. The dependence of α_{crit} on the aspect ratio is shown in Fig. 4(b). It is seen that the problem does not arise when $\alpha > 0.043$ for any value of γ. Additionally, as α decreases, the range of "critical" values of γ becomes wider (see the region under the line in Fig. 4(b)).
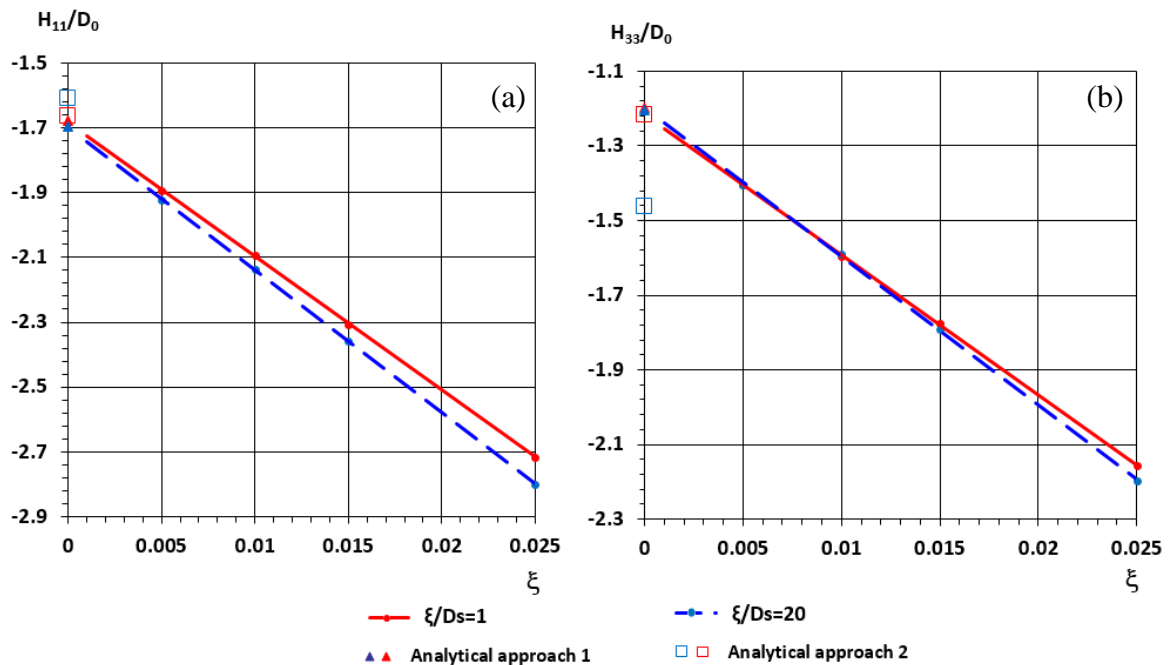

Fig. 4. (a) Dependencies of the dimensionless components of the diffusivity contribution tensor H_{11}/D_0 with respect to the ratio of the diffusivities of the inhomogeneity and the matrix; (b) dependence of the "critical" value the diffusivity ratio with respect to the aspect ratio

Figures 5 and 6 compare the analytical and numerical solutions for the components of the diffusivity contribution tensor. The numerical solution obtained using Numerical method 1 when semi-axes of the inner and outer ellipsoids are related by Eq. (12) is shown. The results are extrapolated to implement the limit transition. Figure 5 presents the results for a material with parameters $\gamma = 2$, $\alpha = 0.1$. In this case, the dependencies H_{11} on R obtained within the framework of the two analytical approaches exhibit similar behavior, with their magnitudes increasing as R increases. It is seen that an increase in R results in a greater contribution of inhomogeneity with an imperfect interface estimated within numerical approach. The results calculated using Analytical model 1 are closer to the numerical results than those obtained from Analytical model 2. This may be due to

the fact that the dependency of the components of the property contribution tensors on R is less pronounced in the case of Analytical model 1 and in the numerical solution. It appears that Analytical model 2 can be used for small values of R, which holds true for small values in the limit $\lim\limits_{\xi \to 0, D_s \to 0} \xi/D_s$.
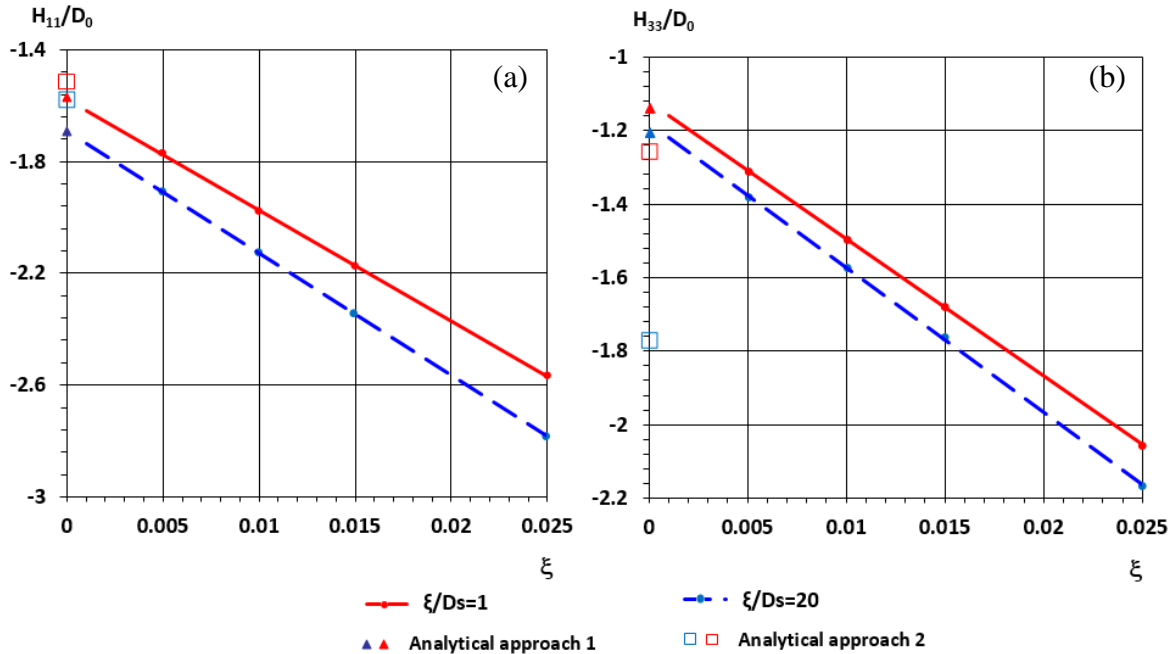
Fig. 5. Extrapolation of the dependencies of the dimensionless components of the diffusivity contribution tensor H_{11}/D_0 (a) and H_{33}/D_0 (b) with respect to the parameter ξ at $\gamma = 2$, $\alpha = 0.1$

Fig. 6. Extrapolation of the dependencies of the dimensionless components of the diffusivity contribution tensor H_{11}/D_0 (a) and H_{33}/D_0 (b) with respect to the parameter ξ at $\gamma = 2$, $\alpha = 0.01$

(a)

(b)
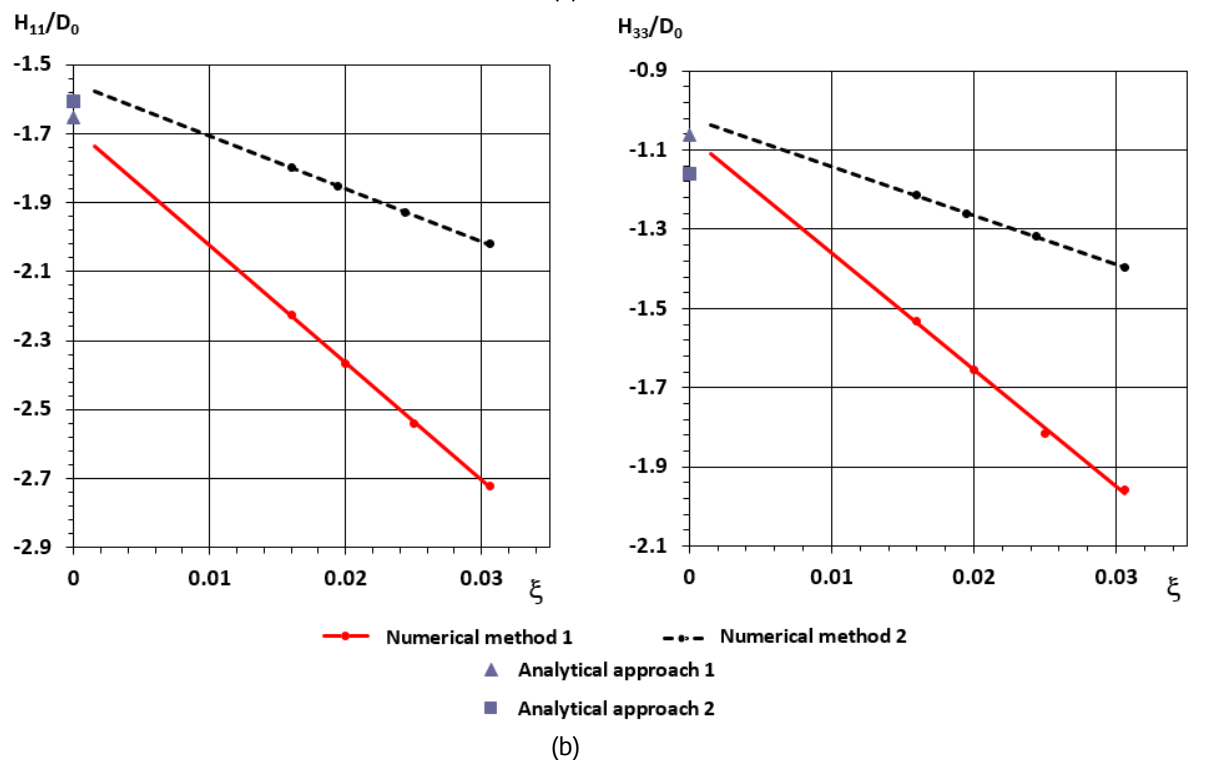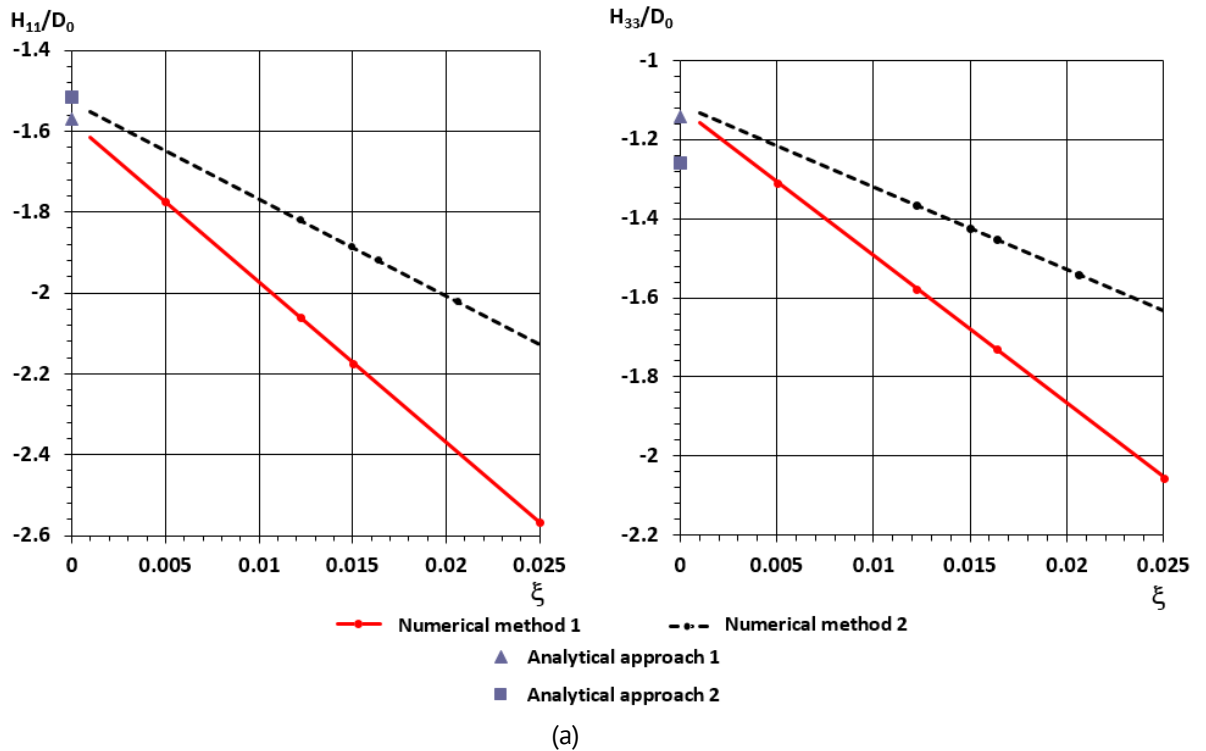
Fig. 7. Comparison of numerical methods at $\gamma = 2$ (a) and $\gamma = 3$ (b) at $\xi/D_s = 1$

Figure 7 compares the results obtained from different numerical methods: Numerical method 1, which introduces the coating using a constant parameter ξ, and Numerical method 2, which introduces the coating through a constant thickness δ along the inhomogeneity boundary. Both approaches yield similar results, allowing either model to be used for simulating an ultra-thin coating. However, the analysis of a layer

with constant thickness results in outcomes that are less dependent on the absolute thickness.

Notably, for a slightly elongated spheroid with $\gamma = 2$, the results obtained within the framework of Numerical method 1.2 using a constant thickness δ along the inhomogeneity axes, coincide with those from Numerical method 2 applying the same constant thickness δ across the entire inhomogeneity boundary, with the difference being less than 1 %. The distinction between these two cases becomes apparent at larger values of γ, as shown in Fig. 8. It is seen that increasing the aspect ratio of spheroidal inhomogeneity leads to a greater difference between Numerical method 1.2 and Numerical method 2 (the value of $\left|H_{ii}^{\mathrm{NM1.2}} - H_{ii}^{\mathrm{NM2}}\right|/H_{ii}^{\mathrm{NM2}}$ is shown, where $H_{ii}^{\mathrm{NM1.2}}$ and H_{ii}^{NM2} are components of H_{ii} calculated within the framework of Numerical method 1.2 and Numerical method 2 respectively).
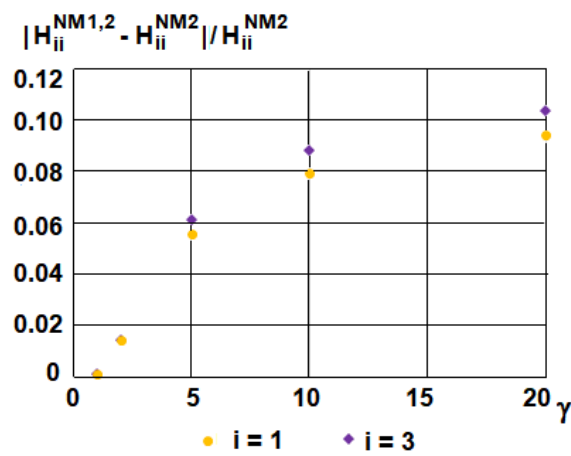
Fig. 8. Dependencies of the slot-relative difference between the components of the diffusivity contribution tensor calculated using Numerical method 1.2 and Numerical method 2 with respect to the aspect ratio of spheroidal inhomogeneity

In summary, the analytical approach that incorporates segregation via prescription of a jump in concentration shows advantages over the alternative method that models segregation through inhomogeneity with a mass isolating coating. The first analytical approach effectively describes segregation both inside and outside inhomogeneities, avoids unphysical outcomes across various internal structure parameters, and yields results that align more closely with numerical findings. Additionally, we have confirmed that our developed numerical methods are capable of accurately simulating segregation occurring outside of inhomogeneities.

Conclusions

Various analytical approaches and numerical methods that account for segregation when determining the effective diffusivity of micro-heterogeneous materials were compared in the paper based on evaluating the diffusivity contribution tensors of individual inhomogeneities. Two analytical approaches and one numerical approach were utilized. In the first analytical approach, segregation was modeled by introducing a concentration jump characterized by a constant segregation parameter. In the second analytical

approach and the numerical approach, segregation was addressed by considering inhomogeneities with a mass-isolating ultra-thin coating. Moreover, in the framework of the numerical approach, different methods of simulating the coating were applied: the layer formed by two ellipsoids and the layer of constant thickness were both considered

The comparison of analytical and numerical solutions demonstrated that the first analytical approach offers more advantages than the second one. This is because it enables the description of segregation in materials with diverse internal structures and provides results that closely match numerical findings, despite its simplicity. Additionally, the developed numerical methods can be further employed to calculate the effective properties of materials with inhomogeneities featuring real mass-isolating coatings of finite thickness and inhomogeneities with irregular shapes.

References

1. Ahn DC, Sofronis P, Dodds R. Modeling of hydrogen-assisted ductile crack propagation in metals and alloys. *International Journal of Fracture.* 2007;145: 135–157.

2. Indeitsev DA, Semenov BN. About a model of structural-phase transformations under hydrogen influence. *Acta Mechanica.* 2008;195: 295–304.

3. Belyaev AK, Polyanskiy VA, Yakovlev YA. Stresses in a pipeline affected by hydrogen. *Acta Mechanica.* 2012;223(8): 1611–1619.

4. Polyanskiy VA, Frolova KP, Sedova YS, Yakovlev YA, Belyaev AK. Behavior of Pipeline Steels in Gaseous Hydrogen-Containing Mixtures. In: Polyanskiy VA., Belyaev AK. (eds.) *Mechanics and Control of Solids and Structures.* Cham: Springer;2022. p.535–556.

5. Sedova YS, Polyanskiy VA, Belyaev AK, Yakovlev YA. Modeling the skin effect, associated with hydrogen charging of samples, within the framework of the HEDE mechanism of cracking. *Materials Physics and Mechanics.* 2023;51(6): 152–159.

6. Herzig C, Mishin Y. Grain boundary diffusion in metals. In: Heitjans P, Kärger J. (eds.) *Diffusion in Condensed Matter.* Berlin: Springer; 2005. p.337–366.

7. Zhang X, Qiao L, Zhang H, Wang P. Influence of impurity gas seeding into deuterium plasma on the surface modification, sputtering erosion and deuterium retention in W and W-La2O3 alloy. *International Journal of Hydrogen Energy.* 2023;48(6): 2075–2089.

8. Zhang Y, Liu L. On diffusion in heterogeneous media. *American Journal of Science.* 2012;312(9): 1028–1047.

9. Markov KZ. Elementary micromechanics of heterogeneous media. In: Markov K, Preziosi L. (eds.) *Heterogeneous Media. Modeling and Simulation in Science, Engineering and Technology.* Boston, MA: Birkhäuser; 2000. p.1–162.

10. Javili A, Kaessmair S, Steinmann P. General imperfect interfaces. *Computer Methods in Applied Mechanics and Engineering.* 2014;275: 76–97.

11. Kaur I, Mishin Y, Gust W. *Fundamentals of Grain and Interphase Boundary Diffusion*. Wiley; 1995.

12. Kalnin JR, Kotomin EA, Maier J. Calculations of the effective diffusion coefficient for inhomogeneous media. *Journal of Physics and Chemistry of Solids.* 2002;63(3): 449–456.

13. Belova IV, Murch GE. Calculation of the effective conductivity and diffusivity in composite solid electrolytes. *Journal of Physics and Chemistry of Solids.* 2005;66(5): 722–728.

14. Knyazeva AG, Grabovetskaya GP, Mishin IP, Sevostianov I. On the micromechanical modelling of the effective diffusion coefficient of a polycrystalline material. *Philosophical Magazine.* 2015;95(19): 2046–2066.

15. Umbanhowar PB, Lueptow RM, Ottino JM. Modeling segregation in granular flows. *Annual Review of Chemical and Biomolecular Engineering.* 2019;10: 129–153.

16. Frolova KP, Vilchevskaya EN. Effective diffusivity of transversely isotropic material with embedded pores. *Materials Physics and Mechanics.* 2021;47(6): 937–950.

17. Miloh T, Benveniste Y. On the effective conductivity of composites with ellipsoidal inhomogeneities and highly conducting interfaces. *Proceedings of the Royal Society of London. Series A: Mathematical, Physical and Engineering Sciences.* 1999;455(1987): 2687–2706.

18. Duan HL, Karihaloo BL. Effective thermal conductivities of heterogeneous media containing multiple imperfectly bonded inclusions. *Physical Review B — Condensed Matter and Materials Physics.* 2007;75(6): 064206.

19. Le Quang H, Pham DC, Bonnet G, He QC. Estimations of the effective conductivity of anisotropic multiphase composites with imperfect interfaces. *International Journal of Heat and Mass Transfer.* 2013;58(1-2): 175–187.

20. Kushch VI., Sevostianov I, Belyaev AS. Effective conductivity of spheroidal particle composite with imperfect interfaces: Complete solutions for periodic and random micro structures. *Mechanics of Materials.* 2015;89: 1–11.

21. Pham DC, Nguyen TK. Thermal conductivity in spherical and circular inclusion composites with highly- and lowly-conducting imperfect interfaces. *International Journal of Heat and Mass Transfer.* 2022;196: 123245.

22. Kushch VI, Mogilevskaya SG. Higher order imperfect interface models of conductive spherical interphase. *Mathematics and Mechanics of Solids.* 2022;29(12): 2386–2410.

23. Endres AL, Knight RJ. A model for incorporating surface phenomena into the dielectric response of a heterogeneous medium. *Journal of Colloid and Interface Science*. 1993;157(2): 418–425.

24. Levin V, Markov M. Effective thermal conductivity of micro-inhomogeneous media containing imperfectly bonded ellipsoidal inclusions. *International Journal of Engineering Science.* 2016(109): 202–215.

25. Markov M, Levin V, Markova I. Determination of effective electromagnetic parameters of concentrated suspensions of ellipsoidal particles using Generalized Differential Effective Medium approximation. *Physica A: Statistical Mechanics and its Applications.* 2018;492: 113–122.

26. Kachanov M, Sevostianov I. Micromechanics of materials, with applications. In: *Solid Mechanics and Its Applications.* Cham: Springer; 2018. p.249.

27. Eshelby JD. Elastic inclusions and inhomogeneities. In: *Collected works of JD Eshelby.* Dordrecht: Springer; 2006. p.297–350.

28. Fricke H. A mathematical treatment of the electric conductivity and capacity of disperse systems I. The electric conductivity of a suspension of homogeneous spheroids. *Physical Review*. 1924;24(5): 575.

29. Frolova KP, Vilchevskaya EN, Polyanskiy VA. Modeling of Imperfect Contacts in Determining the Effective Diffusion Permeability. *Vestnik St. Petersburg University, Mathematics.* 2023;56(4): 459–469.

30. Frolova KP, Vilchevskaya EN. Comparison of approaches to accounting for imperfect contacts when determining the effective permeability of material. *St. Petersburg State Polytechnical University Journal. Physics and Mathematics.* 2023;16(4): 146–159.

31. Eberly D. *Distance from a point to an ellipse, an ellipsoid, or a hyperellipsoid*. 2011.

32. Pope SB. *Algorithms for ellipsoids*. 2008.

33. Yanenko NN. Simple Schemes in Fractional Steps for the Integration of Parabolic Equations. In: Holt M. (ed.) *The Method of Fractional Steps.* Berlin: Springer; 1971. p.17–41.

About Authors

Ksenia P. Frolova 🆔 Sc

Candidate of Physico-Mathematical Sciences
Senior Researcher (Institute for Problems in Mechanical Engineering RAS, St. Petersburg, Russia)

Nikolay M. Bessonov 🆔 Sc

Doctor of Physico-Mathematical Sciences
Chief Researcher (Institute for Problems in Mechanical Engineering RAS, St. Petersburg, Russia)

Elena N. Vilchevskaya 🆔 Sc

Doctor of Physico-Mathematical Sciences
Associate Professor (Flugsnapparegatan 6, Mölndal, Sweden)

Appendix A. Numerical procedure

To solve Eq. (1) for concentration, we employed an implicit numerical procedure based on the Alternating Direction Implicit (ADI) algorithm [33].

We can express Eq. (1) for concentration in symbolic form as follows:

$$L(c) = 0, \tag{A.1}$$

where L is a differential operator defined in Cartesian coordinates (x, y, z) as

$$L = \frac{\partial}{\partial x}\left(D(\mathbf{r})\frac{\partial}{\partial x}\right) + \frac{\partial}{\partial y}\left(D(\mathbf{r})\frac{\partial}{\partial y}\right) + \frac{\partial}{\partial z}\left(D(\mathbf{r})\frac{\partial}{\partial z}\right) \equiv L_1 + L_2 + L_3.$$

To find the solution of Eq. (A.1), we treat it as the stationary solution of the unsteady equation using an implicit scheme:

$$\frac{\xi^{n+1}}{\tau} = L(c^{n+1}), \tag{A.2}$$

where $\xi^{n+1} = c^{n+1} - c^n$, τ is a "pseudo-time" step, n is the iteration number.

Equation (A.2) can be rewritten in the following manner:

$$\frac{\xi^{n+1}}{\tau} = L(c^n) + L(\xi^{n+1}). \tag{A.3}$$

Equation (A.3), in turn, is convenient to rewrite as:

$$(I - \tau L)\xi^{n+1} = \tau L(c^n), \tag{A.4}$$

where I is the identity operator.

Equation (A.4) can be factored in the following way:

$$(I - \tau L_1)(I - \tau L_2)(I - \tau L_3)\xi^{n+1} = \tau L(c^n) + O(\xi^{n+1}). \tag{A.5}$$

Then the main steps of algorithm are as follows:

$$\begin{cases} \text{Step 1:} & \xi^n = \tau L(c^n) \\ \text{Step 2:} & (I - \tau L_1)\xi^{n+1/3} = \xi^n \\ \text{Step 3:} & (I - \tau L_2)\xi^{n+2/3} = \xi^{n+1/3} \\ \text{Step 4:} & (I - \tau L_3)\xi^{n+1} = \xi^{n+2/3} \\ \text{Step 5:} & c^{n+1} = c^n + \xi^{n+1} \end{cases} \tag{A.6}$$

Appendix B. Calculating the distance between point and ellipsoid surface

The distance between a point and the surface of an ellipsoid can be expresses as the length of the normal vector dropped from the given point onto the ellipsoidal surface. The surface of the ellipsoid in Cartesian coordinates (x, y, z) is defined be the equation:

$$\left(\frac{x}{a_1}\right)^2 + \left(\frac{y}{a_2}\right)^2 + \left(\frac{z}{a_3}\right)^2 = 1, \tag{B.1}$$

where a_1, a_2, a_3 are the semi-axes of the ellipsoid.

We first discuss the problem of determining the position of some point along the normal vector to ellipsoid's surface. Let this point be located at a given distance δ to a point on the ellipsoid's surface represented by the position vector $\mathbf{r} = x\mathbf{e}_1 + y\mathbf{e}_2 + z\mathbf{e}_3$. The unit external normal vector $\mathbf{n}$ to the ellipsoid's surface at the point $\mathbf{r}$ can be defined as:

$$\mathbf{n} = \frac{\frac{x}{a_1^2}}{\sqrt{\left(\frac{x}{a_1^2}\right)^2 + \left(\frac{y}{a_2^2}\right)^2 + \left(\frac{z}{a_3^2}\right)^2}}\mathbf{e}_1 + \frac{\frac{y}{b_1^2}}{\sqrt{\left(\frac{x}{a_1^2}\right)^2 + \left(\frac{y}{a_2^2}\right)^2 + \left(\frac{z}{a_3^2}\right)^2}}\mathbf{e}_2 + \frac{\frac{z}{c_1^2}}{\sqrt{\left(\frac{x}{a_1^2}\right)^2 + \left(\frac{y}{a_2^2}\right)^2 + \left(\frac{z}{a_3^2}\right)^2}}\mathbf{e}_3. \tag{B.2}$$

Let $\mathbf{r}_0 = x_0\mathbf{e}_1 + y_0\mathbf{e}_2 + z_0\mathbf{e}_3$ be the sought-for position-vector. Its coordinates can be determined from the following equations:

$$x_0 = x + \frac{\frac{x}{a_1^2}}{\sqrt{\left(\frac{x}{a_1^2}\right)^2 + \left(\frac{y}{a_2^2}\right)^2 + \left(\frac{z}{a_3^2}\right)^2}}\,\delta$$

$$y_0 = y + \frac{\frac{y}{b_1^2}}{\sqrt{\left(\frac{x}{a_1^2}\right)^2 + \left(\frac{y}{a_2^2}\right)^2 + \left(\frac{z}{a_3^2}\right)^2}}\,\delta. \tag{B.3}$$

$$z_0 = z + \frac{\frac{z}{c_1^2}}{\sqrt{\left(\frac{x}{a_1^2}\right)^2 + \left(\frac{y}{a_2^2}\right)^2 + \left(\frac{z}{a_3^2}\right)^2}}\,\delta$$

Returning to the problem of calculating the distance between a specified point and the surface of the ellipsoid, both the distance δ and the coordinates x, y, z are initially unknown. To find these values, we must solve an inverse problem described by the following system of equations:

$$x_0 - \left(1 + \frac{h}{a_1^2\sqrt{\left(\frac{x}{a_1^2}\right)^2 + \left(\frac{y}{a_2^2}\right)^2 + \left(\frac{z}{a_3^2}\right)^2}}\right)x = 0$$

$$y_0 - \left(1 + \frac{y}{b_1^2\sqrt{\left(\frac{x}{a_1^2}\right)^2 + \left(\frac{y}{a_2^2}\right)^2 + \left(\frac{z}{a_3^2}\right)^2}}h\right)y = 0 \tag{B.4}$$

$$z_0 - \left(1 + \frac{z}{c_1^2\sqrt{\left(\frac{x}{a_1^2}\right)^2 + \left(\frac{y}{a_2^2}\right)^2 + \left(\frac{z}{a_3^2}\right)^2}}h\right)z = 0$$

$$\left(\frac{x}{a_1}\right)^2 + \left(\frac{y}{a_2}\right)^2 + \left(\frac{z}{a_3}\right)^2 - 1 = 0$$

Solution of the system of Eqs. (B.4) was found in the present research numerically.